Non-linear modeling of storage and damping rings using symplectic integrators

Yannis PAPAPHILIPPOU

May 26th-28th, 2008

Outline

- Contributors:
  - Ch. Skokos (MPI, Dresden), J. Laskar (IMCEE), E. Levichev, P. Piminov (BINP), F. Zimmermann (CERN), M. Korostelev (Cockroft Inst.)

- Acknowledgements
  - H. Braun (CERN), L. Nadolski (Soleil), P. Robutel (IMCEE)

Outline

- Symplectic integration
  - The SABA2 integrator
  - Application to the ESRF storage ring ideal lattice
- Compact Linear Collider (CLIC) damping rings
  - Design challenges
  - Sextupole scheme
  - Tune scans
  - Wiggler effect
  - Effect of radiation damping

Symplectic integration

Laskar and Robutel Cel. Mech Dyn Astr. 80, 39, 2001

- Symplectic integrators with positive steps for Hamiltonian systems $H = A + \epsilon B$ with both *A* and *B* integrable
- Consider Hamiltonian system $H(\vec{p}, \vec{q})$, with ***N*** degrees of freedom
- A trajectory of the system in phase space is described by

$$\vec{x}(t) = (x_1(t), \ldots, x_{2N}(t)),\ x_i = p_i,\ x_{i+N} = q_i,\ i = 1, \ldots, N$$

- Hamilton's equations of motion take the form

$$\frac{d\vec{x}}{dt} = \{H, \vec{x}\} = L_H \vec{x},$$

with the usual Poisson brackets $\{f, g\} = \sum_{i=1}^{N} \left(\frac{\partial f}{\partial p_i} \frac{\partial g}{\partial q_i} - \frac{\partial f}{\partial q_i} \frac{\partial g}{\partial p_i} \right).$

- The solution is formally written as

$$\vec{x}(t) = \sum_{n \geq 0} \frac{t^n}{n!} L_H^n \vec{x}(0) = e^{tL_H} \vec{x}(0).$$

SABA$_2$ integrator

- A symplectic integrator of order *n* from t to $t+\tau$ consists of approximating the operator $e^{\tau L_H} = e^{\tau(L_A + L_{\epsilon B})}$ by products of $e^{c_i \tau L_A}$ and $e^{d_i \tau L_{\epsilon B}}$, $i = 1, \ldots, n$ which integrate exactly *A* and *B* over the time-spans $c_i\tau$ and $d_i\tau$
- The constants c_i and d_i are chosen for reducing the error
- The SABA$_2$ integrator is written as

$$\mathrm{SABA}_2 = e^{c_1\tau L_A} e^{d_1 \tau L_{\epsilon B}} e^{c_2 \tau L_A} e^{d_1 \tau L_{\epsilon B}} e^{c_1 \tau L_A},$$

with $c_1 = \frac{1}{2}\left(1 - \frac{1}{\sqrt{3}}\right)$, $c_2 = \frac{1}{\sqrt{3}}$, $d_1 = \frac{1}{2}$.

- When $\{\{A, B\}, B\}$ is integrable, e.g. when *A* is quadratic in momenta and *B* depends only in positions, the accuracy of the integrator is improved by two small negative steps

$$\mathrm{SABA}_2\mathrm{C} = e^{-\tau^3 \epsilon^2 \frac{c}{2} L_{\{\{A,B\},B\}}} \left(\mathrm{SABA}_2\right) e^{-\tau^3 \epsilon^2 \frac{c}{2} L_{\{\{A,B\},B\}}}$$

with $c = (2 - \sqrt{3})/24$

Performance of $SABA_2$

- The accuracy of the $SABA_2C$ was proved an order of magnitude more precise than the Forest-Ruth 4th order integrator

Nadolski and Laskar, EPAC 2002

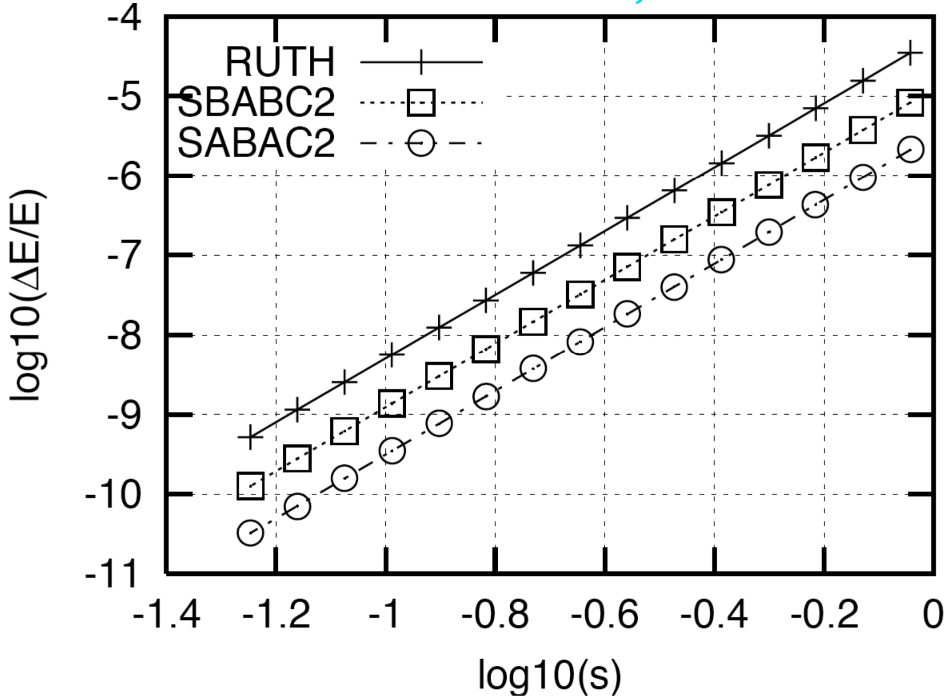

- Note finally that the usual “drift-kick” scheme corresponds to the 2nd order integrator of this class

$$\mathrm{SABA}_1 = e^{\frac{\tau}{2} L_A} e^{\tau L_{\epsilon B}} e^{\frac{\tau}{2} L_A},$$

SABA$_2$C for accelerators

- The accelerator Hamiltonian in the small angle, "hard-edge" approximation is written as $H(x,y,l,p_x,p_y,\delta;s) = H_0 + V,$

  with the unperturbed part $H_0 = (1+h\ x)\dfrac{p_x^2+p_y^2}{2(1+\delta)},$

  and the perturbation $V(x,y) = \displaystyle\sum_{n\geq 1}\sum_{j=0}^{n} a_{n,j}x^j y^{n-j}$

- The unperturbed part of the Hamiltonian can be integrated

$$e^{sL_A} : \left\{\begin{array}{lcl} x^f & = & \dfrac{1}{h}\left\{(1+hx^i)\left(\cos\phi + \dfrac{p_x^i}{p_y^i}\sin\phi\right)^2 - 1\right\} \\ y^f & = & y^i + \dfrac{1+hx^i}{h}\left\{\dfrac{{p_x^i}^2+{p_y^i}^2}{{p_y^i}^2}\phi + \dfrac{{p_y^i}^2-{p_x^i}^2}{2{p_y^i}^2}\sin(2\phi) + 2\dfrac{p_x^i}{p_y^i}\sin^2\phi\right\} \\ p_x^f & = & p_y^i\dfrac{p_x^i - p_y^i\tan\phi}{p_y^i + p_x^i\tan\phi} \\ p_y^f & = & p_y^i \end{array}\right.$$

with $\phi = \dfrac{p_y^i hs}{2(1+\delta)}$

SABA$_2$C for accelerators II

- The perturbation part of the Hamiltonian can be integrated

$$e^{sL_B}:\begin{cases} x^f = x^i \quad , \quad p_x^f = p_x^i - \left.\dfrac{\partial V}{\partial x}\right|_i s & \text{with } \left.\dfrac{\partial V}{\partial x}\right|_i = \displaystyle\sum_{n\geq 1}\sum_{j=1}^{n} j a_{n,j}(x^i)^{j-1}(y^i)^{n-j} \\ y^f = y^i \quad , \quad p_y^f = p_y^i - \left.\dfrac{\partial V}{\partial y}\right|_i s & \left.\dfrac{\partial V}{\partial y}\right|_i = \displaystyle\sum_{n\geq 1}\sum_{j=0}^{n}(n-j)a_{n,j}(x^i)^j(y^i)^{n-j-1} \end{cases}$$

- The corrector is expressed as

$$C = \{\{A,B\},B\} = \frac{1+hx}{1+\delta}\left[\left(\frac{\partial V}{\partial x}\right)^2 + \left(\frac{\partial V}{\partial y}\right)^2\right],$$

and the operator for the corrector is written as

$$e^{sL_C}:\begin{cases} x^f = x^i \\ y^f = y^i \\ p_x^f = p_x^i - \dfrac{1}{1+\delta}\left\{h\left[\left.\dfrac{\partial V}{\partial x}\right|_i^2 + \left.\dfrac{\partial V}{\partial y}\right|_i^2\right] + 2(1+hx^i)\left[\left.\dfrac{\partial V}{\partial x}\right|_i \left.\dfrac{\partial^2 V}{\partial x^2}\right|_i + \left.\dfrac{\partial V}{\partial y}\right|_i \left.\dfrac{\partial^2 V}{\partial x \partial y}\right|_i\right]\right\} s \\ p_y^f = p_y^i - \dfrac{2(1+hx^i)}{1+\delta}\left\{\left.\dfrac{\partial V}{\partial x}\right|_i \left.\dfrac{\partial^2 V}{\partial x\partial y}\right|_i + \left.\dfrac{\partial V}{\partial y}\right|_i \left.\dfrac{\partial^2 V}{\partial y^2}\right|_i\right\} s \end{cases} .$$

Application to the ESRF

- Consider the old ESRF "ideal" lattice, i.e. perfectly symmetric (periodicity of 16) with the only non-linearity coming from the sextupoles
- Integrate the equations of motions with three different methods
  - "Drift-Kick" method by splitting the 0.4m sextupoles in a drift+kick+drift
  - Splitting the sextupoles in 10*(drift+kick)+drift
  - Using the $SABA_2C$ symplectic integrator
- Produce frequency maps by using Laskar's NAFF algorithm and compare

Frequency map I

- Comparison between frequency maps produced by "drift-kick" 1 kick versus 10 kicks

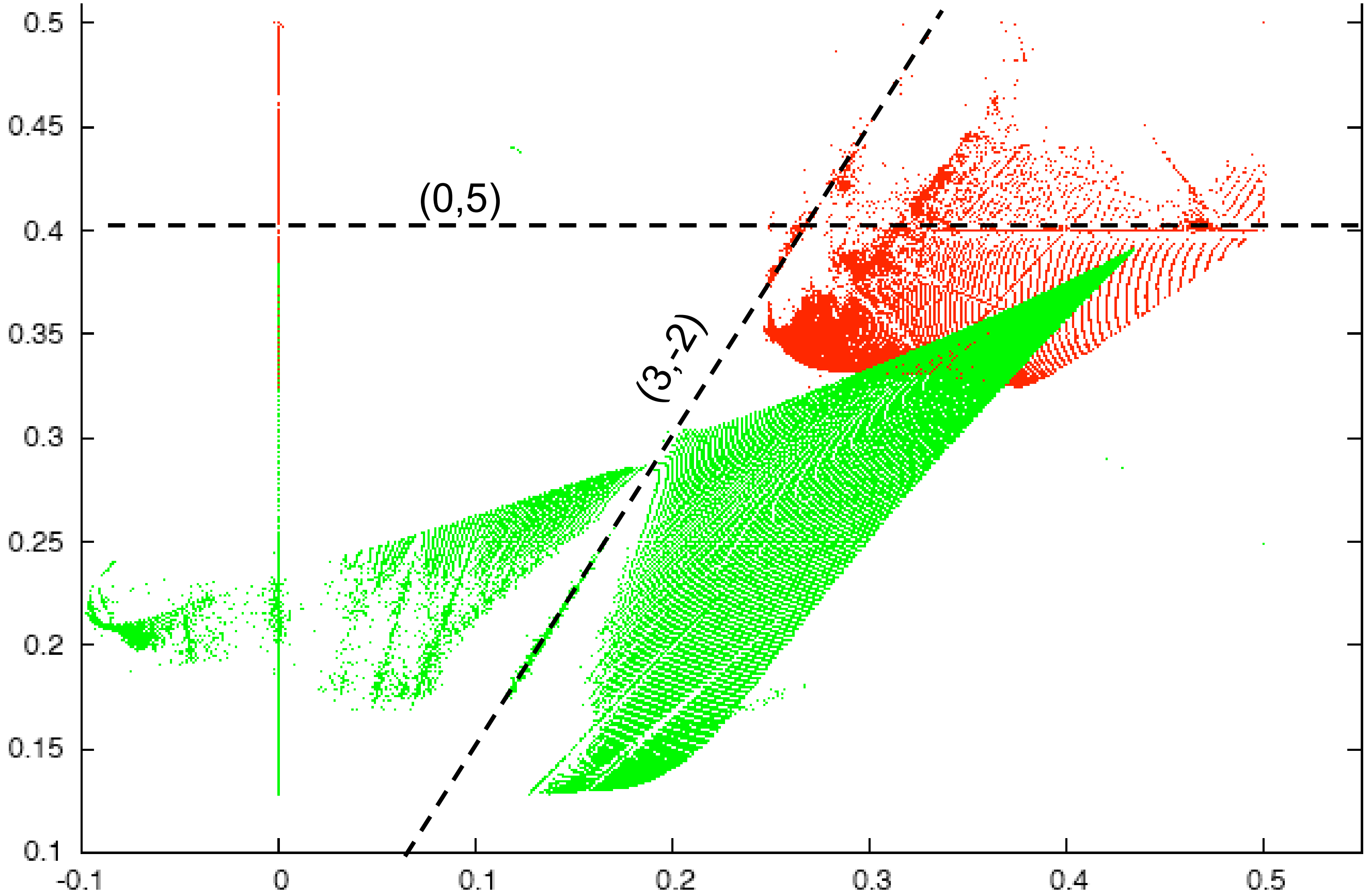

Frequency map II

- Frequency map using the $SABA_2C$ symplectic integrator reproduces the “10-kick” case

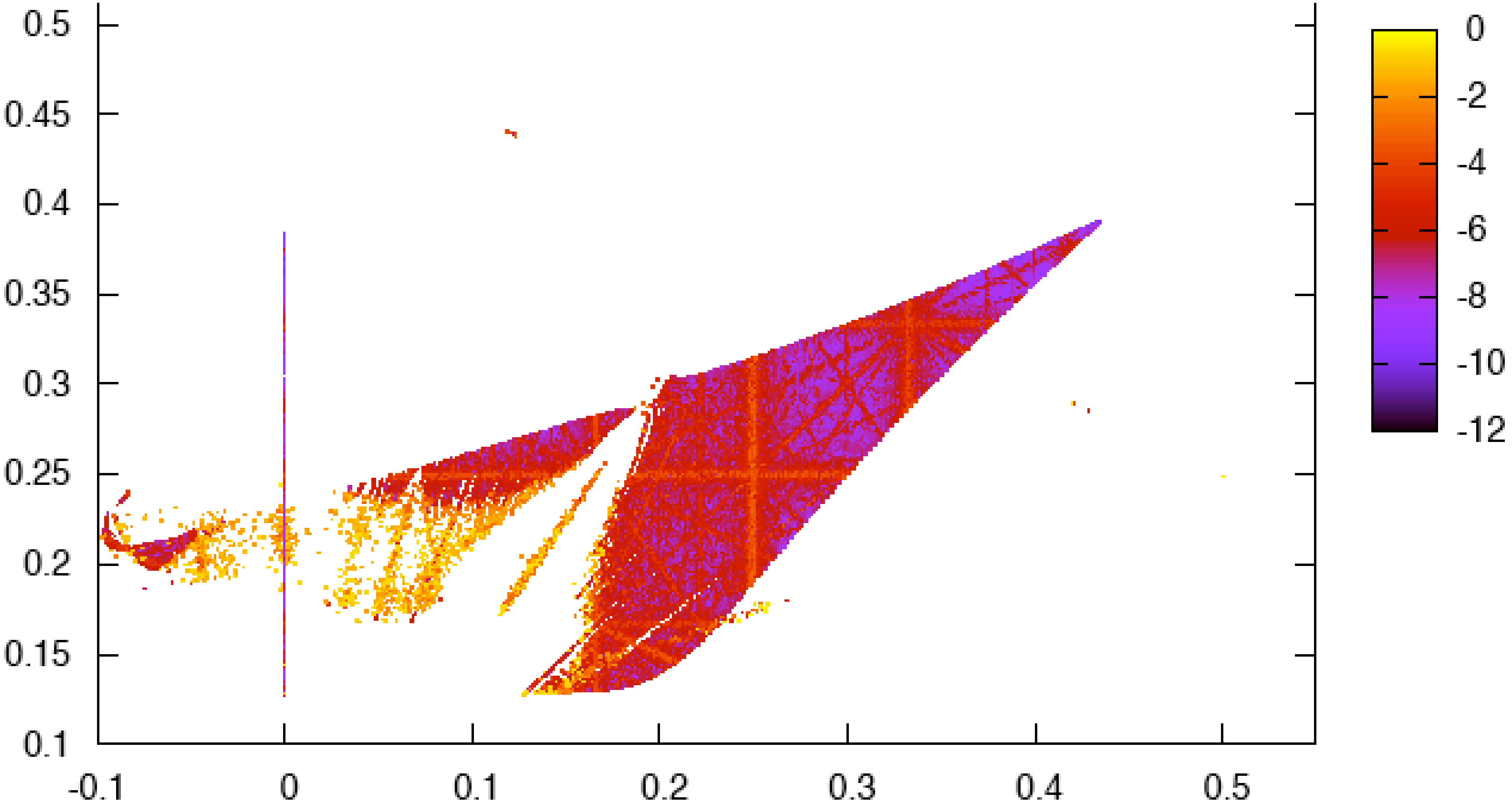

Diffusion maps

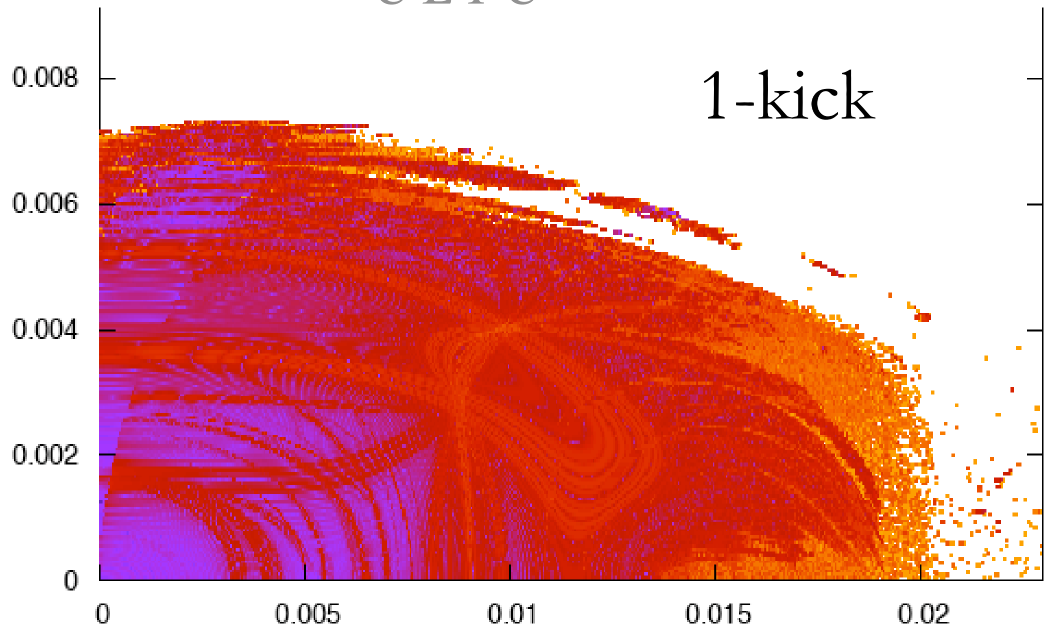

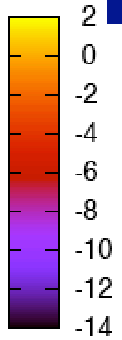

- Colour coding following the logarithm of the diffusion vector amplitude

$$\boldsymbol{D}|_{t=\tau} = \boldsymbol{\nu}|_{t\in(0,\tau/2]} - \boldsymbol{\nu}|_{t\in(\tau/2,\tau]}$$

- Diffusion map using the $SABA_2C$ symplectic integrator shows lower horizontal and slightly higher vertical DA than 1-kick integrator

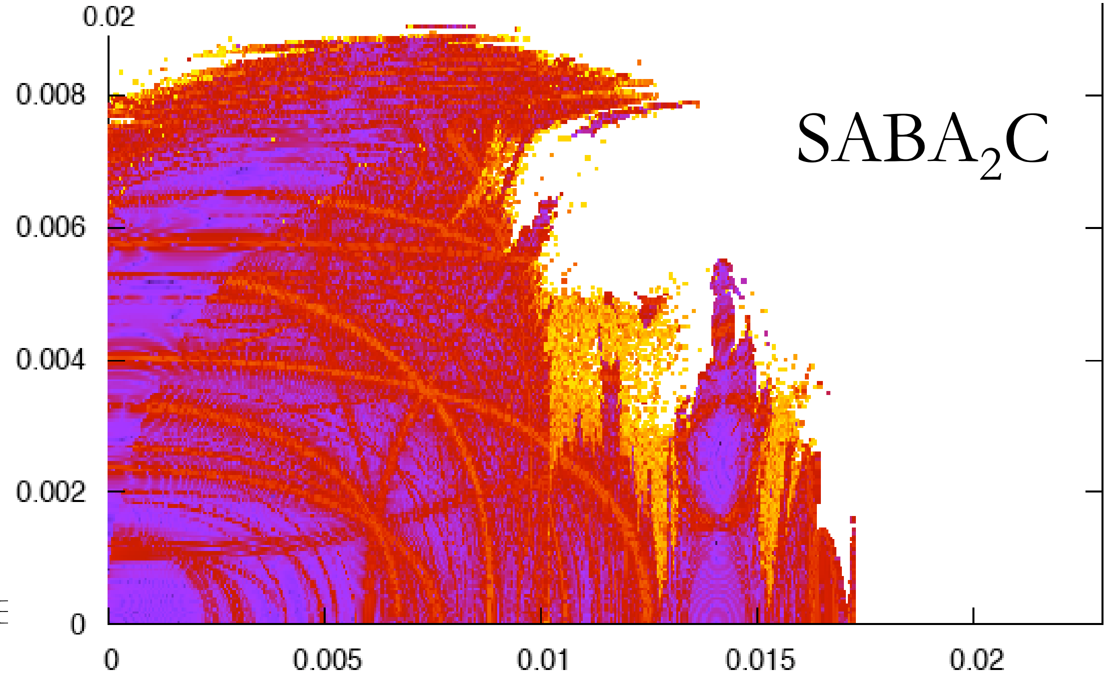

The CLIC Project

- **Compact Linear Collider** : multi-TeV e-p collider for high energy physics beyond the LHC
- Center-of-mass energy from 0.5 to **3 TeV**
- RF gradient and frequencies are **very high**
  - **100 MV/m** in room temperature accelerating structures at **12 GHz**
- **Two-beam-acceleration concept**
  - High current "**drive**" beam, decelerated in power extraction structures (**PETS**), generates RF power for main beam.
- Challenges:
  - Efficient generation of drive beam
  - PETS generating the required power
  - 12 GHz RF structures for the high gradient
  - Generation/preservation of small emittance beam
  - Focusing to nanometer beam size
  - Precise alignment of the different components

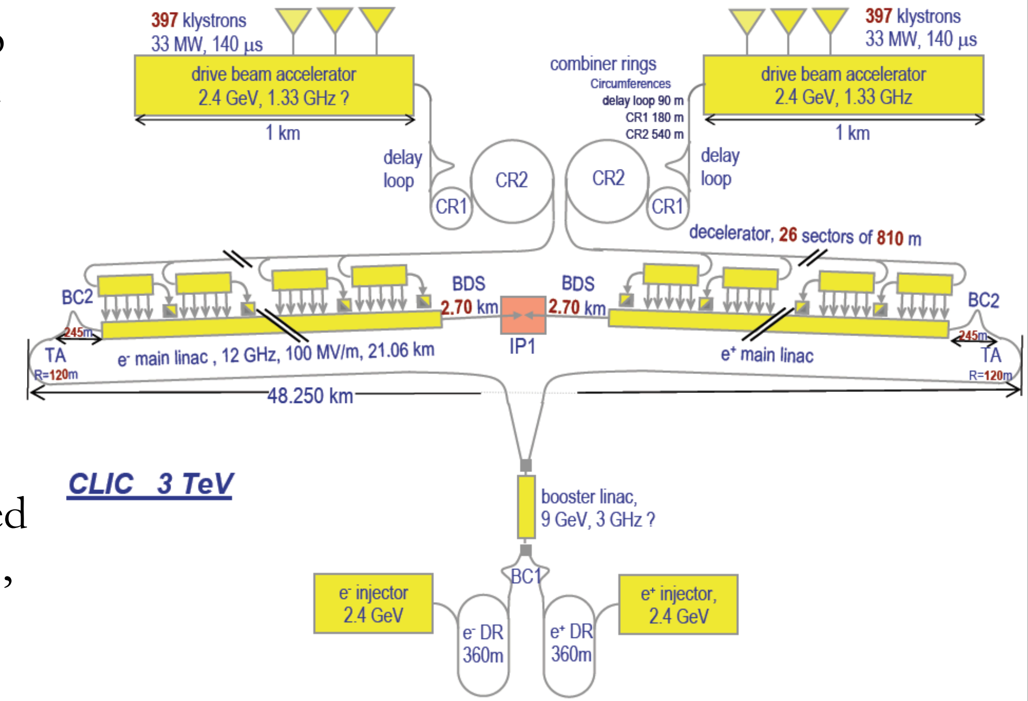

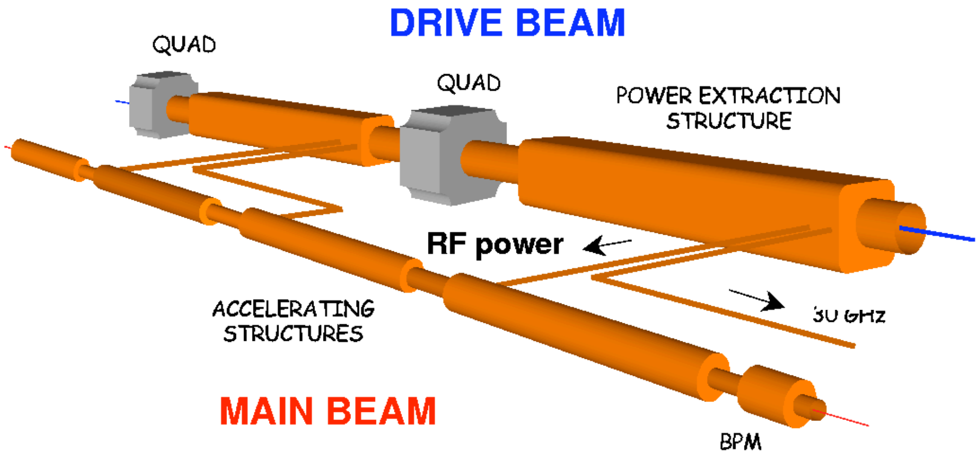

Injector complex

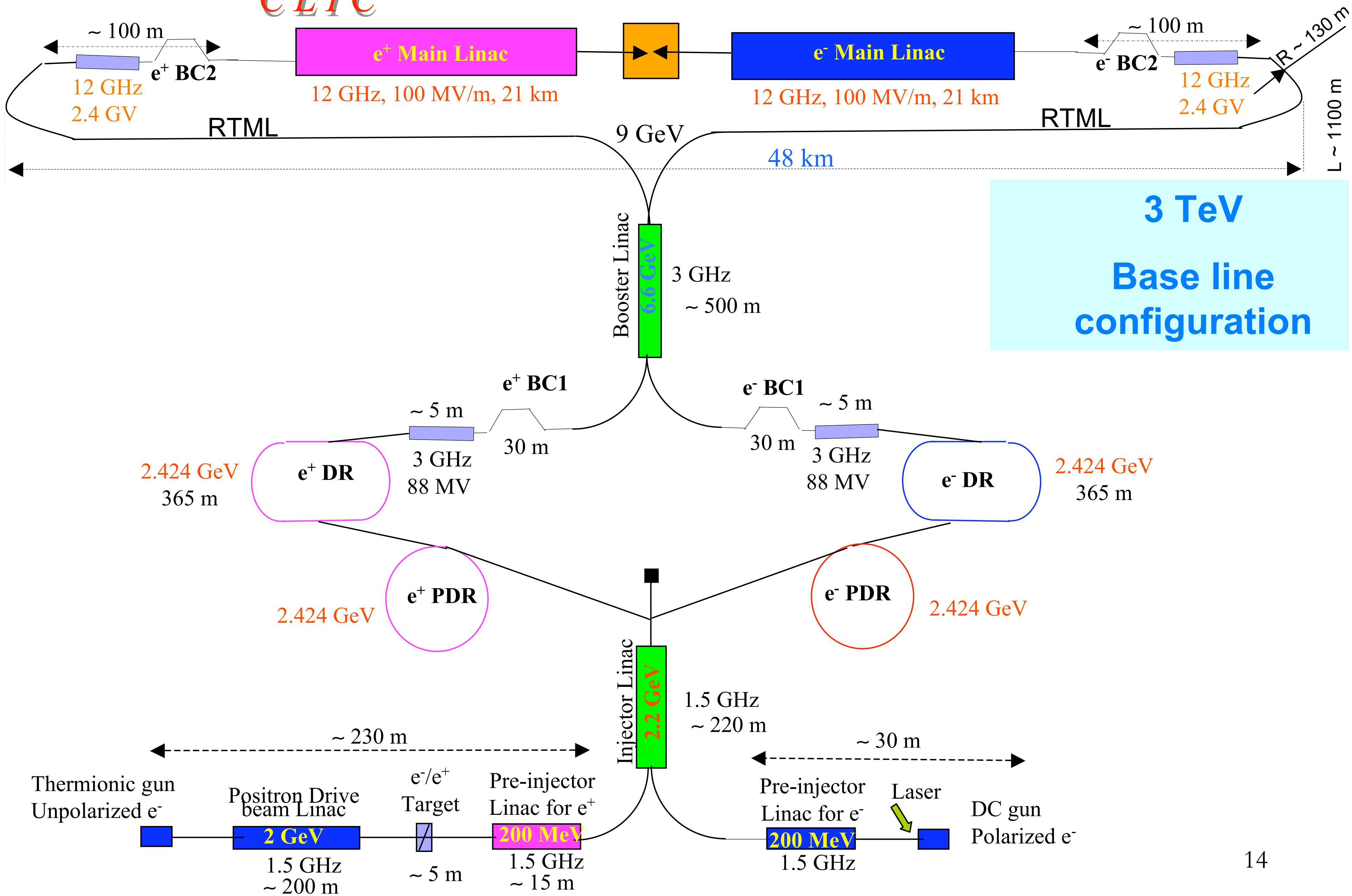

3 TeV

Base line configuration

Damping ring design goals

CLIC

- Ultra-low emittance and high beam polarisation impossible to be produced by conventional particle source:
  - Ring to damp the beam size to desired values through synchrotron radiation
- Intra-beam scattering due to high bunch current blows-up the beam
  - Equilibrium “IBS dominated” emittance should be reached fast to match collider high repetition rate
- Other collective effects (e.g. e^--cloud) may increase beam losses
- Starting parameter dictated by design criteria of the collider (e.g. luminosity), injected beam characteristics or compatibility with the downstream system parameters (e.g. bunch compressors)

PARAMETER	CLIC
bunch population (10^9)	4.1
bunch spacing [ns]	0.5
number of bunches/train	312
number of trains	1
Repetition rate [Hz]	50
Extracted hor. normalized emittance [nm]	<680
Extracted ver. normalized emittance [nm]	< 20
Extracted long. normalized emittance [eV m]	<5000
Injected hor. normalized emittance [μm]	63
Injected ver. normalized emittance [μm]	1.5
Injected long. normalized emittance [keV m]	1240

Horizontal emittance vs. energy

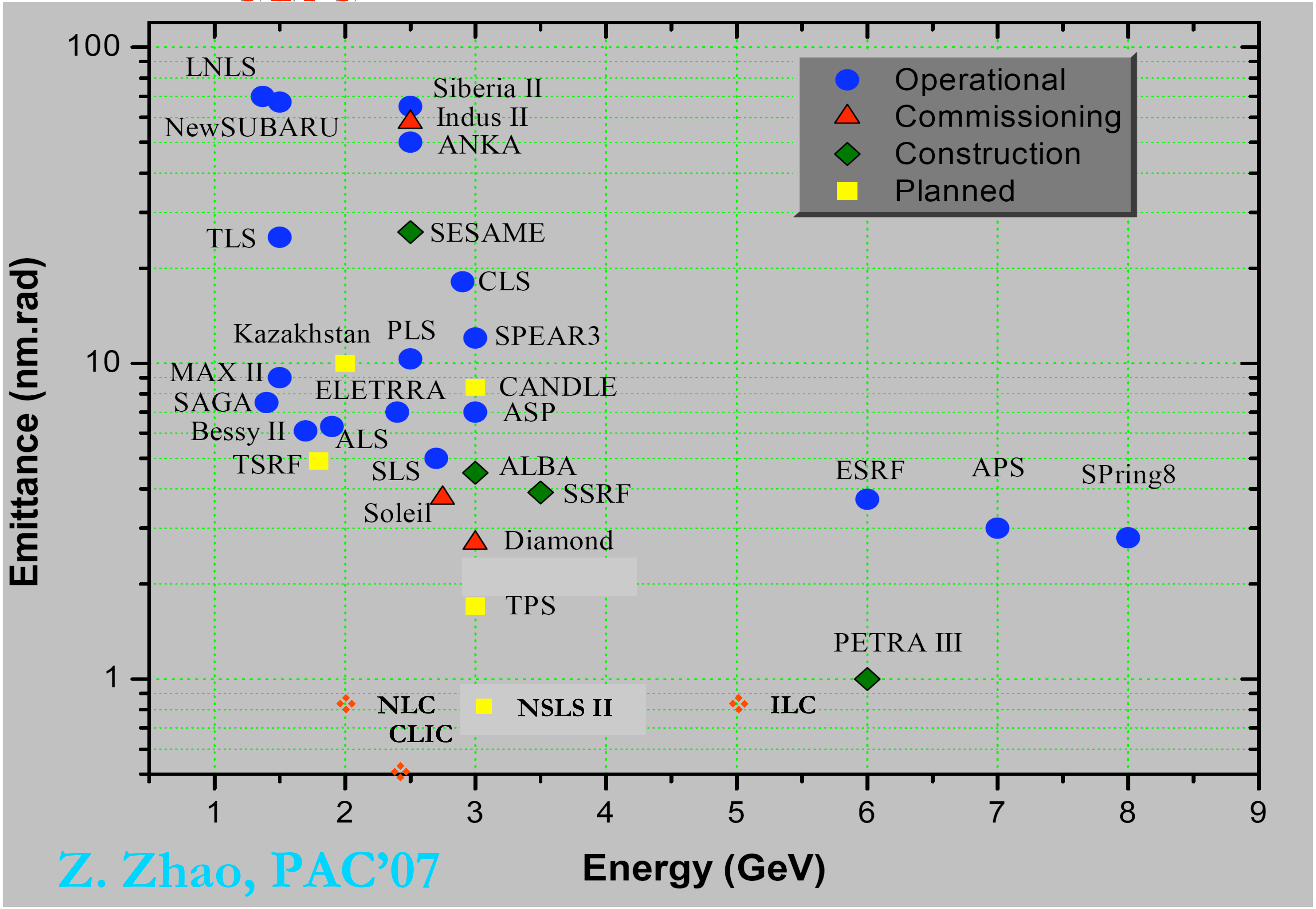

Z. Zhao, PAC'07

Vertical emittance vs. energy

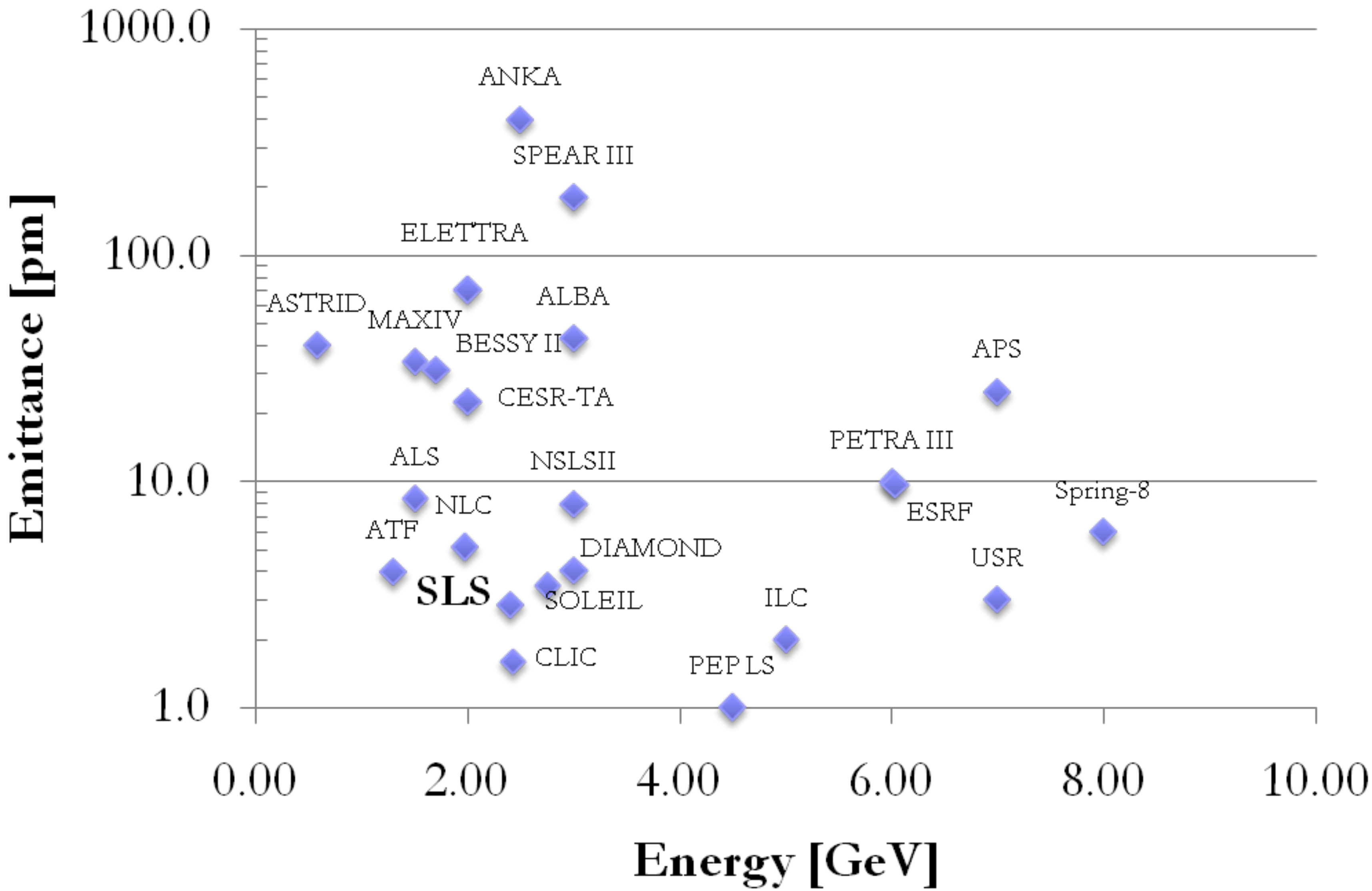

CLIC damping ring layout

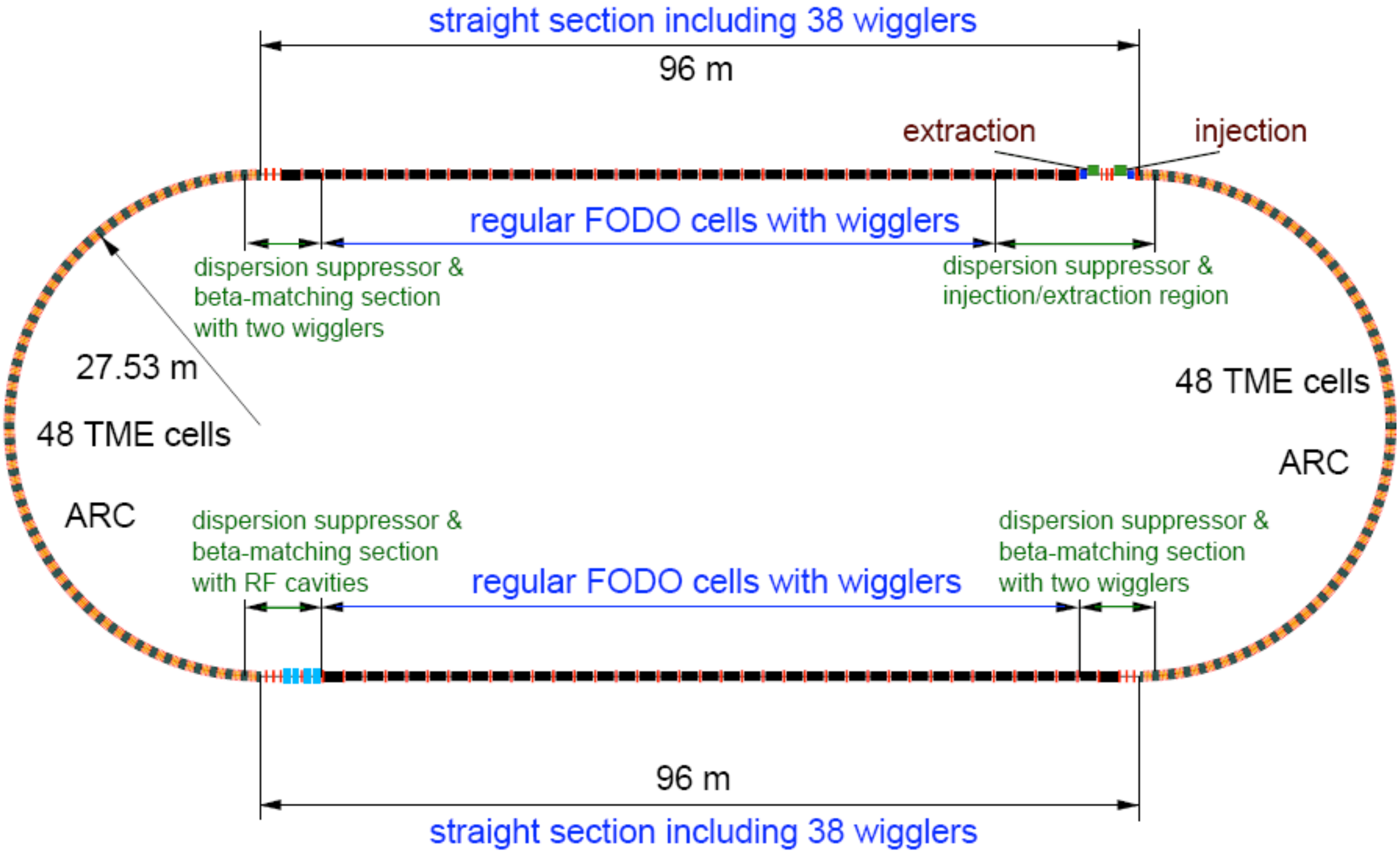

TME arc cell

- TME cell chosen for compactness and efficient emittance minimisation over Multiple Bend Structures (or achromats) used in light sources
- Large phase advance necessary to achieve optimum equilibrium emittance
- Very low dispersion
- Strong sextupoles needed to correct chromaticity
- Impact in dynamic aperture

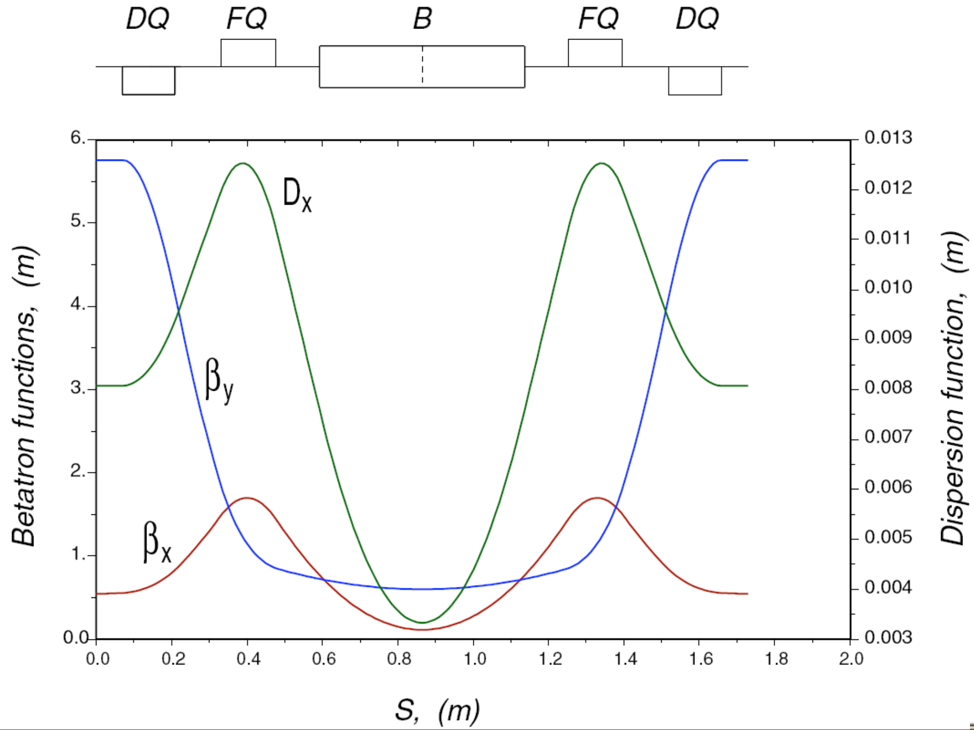

Energy	2.42 GeV
Field of the bending magnet, B_a	0.932 T
Length of the bending magnet	0.545 m
Bending angle	$2\pi/100$
Bending radius	8.67 m
Length of the cell, L_{TME}	1.73 m
Horizontal phase advance, μ_x	210°
Vertical phase advance, μ_y	90°
Emittance detuning factor, ϵ_r	1.8
Horizontal chromaticity, $\partial\nu_x/\partial\delta$	-0.84
Vertical chromaticity, $\partial\nu_y/\partial\delta$	-1.18
Average horizontal beta function, $\langle\beta_x\rangle$	0.847 m
Average vertical beta function, $\langle\beta_y\rangle$	2.22 m
Average horizontal dispersion, $\langle D_x\rangle$	0.0085 m
Relative horizontal beta function, $\beta_r = \beta^*/\beta^*_m$	$0.113/0.07 = 1.6$
Relative horizontal dispersion, $D_r = D^*/D^*_m$	$0.00333/0.00143 = 2.33$

Wigglers' effect with IBS

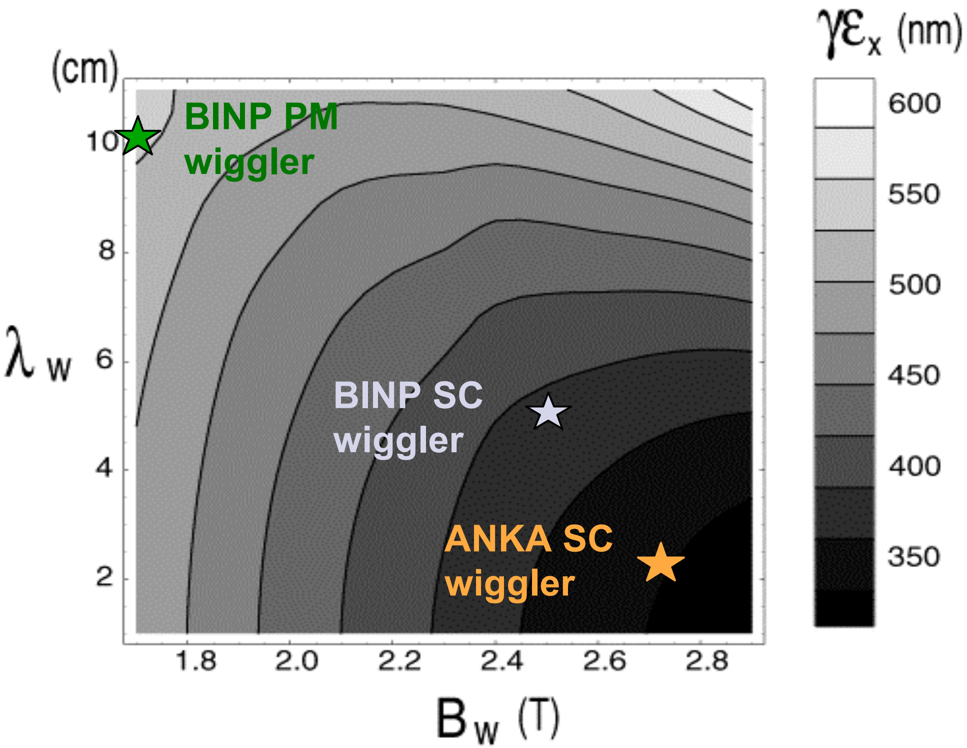

- For higher wiggler field and smaller period the transverse emittance computed with IBS gets smaller
- The longitudinal emittance has a different optimum but it can be controlled with the RF voltage

- The choice of the wiggler parameters is finally dictated by their technological feasibility.
  - Normal conducting wiggler of 1.7T can be extrapolated by existing designs
  - Super-conducting options have to be designed, built and tested

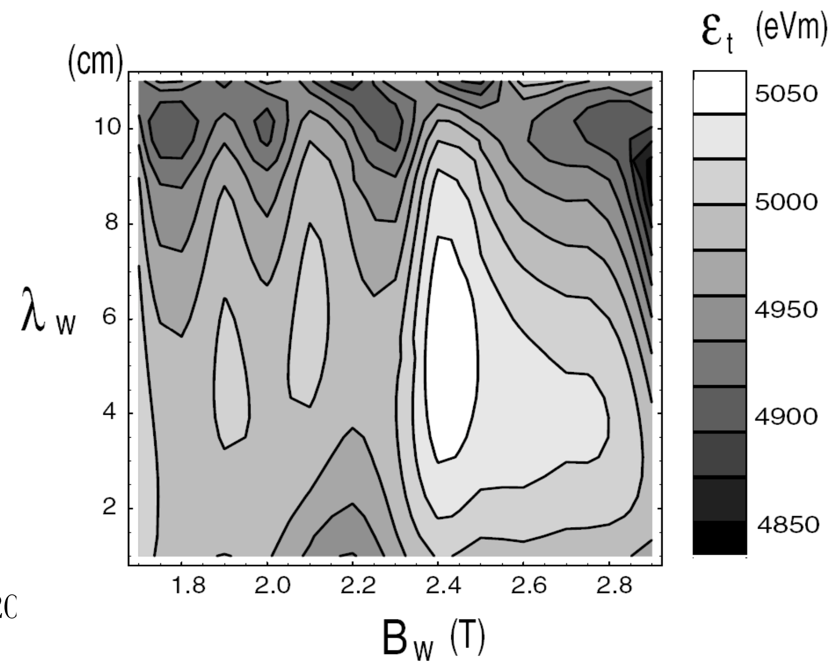

Sextupole scheme

- Two sextupole schemes
  - 2 and 9 families of sextupoles
  - For 2nd scheme sextupoles are separated by a *-I* transformer (2nd order achromat)
- Dynamic aperture is 9σ_x in the horizontal and 14σ_y in the vertical plane (comfortable for injection)

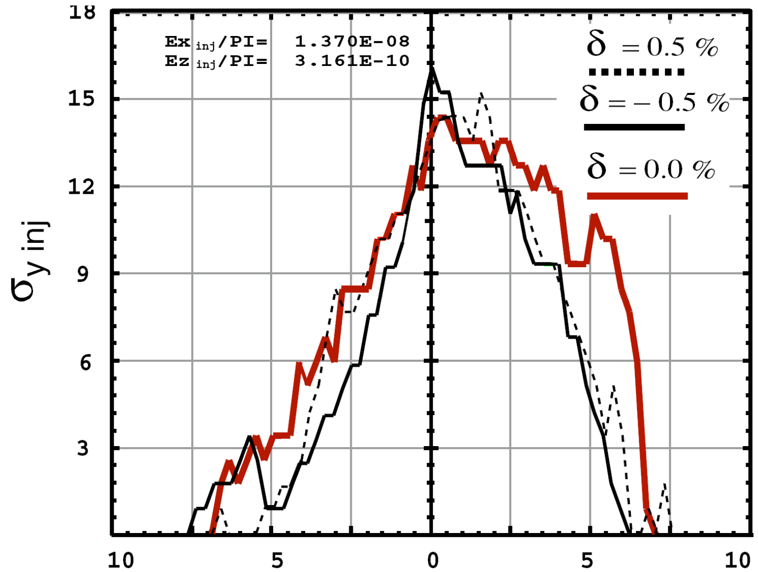

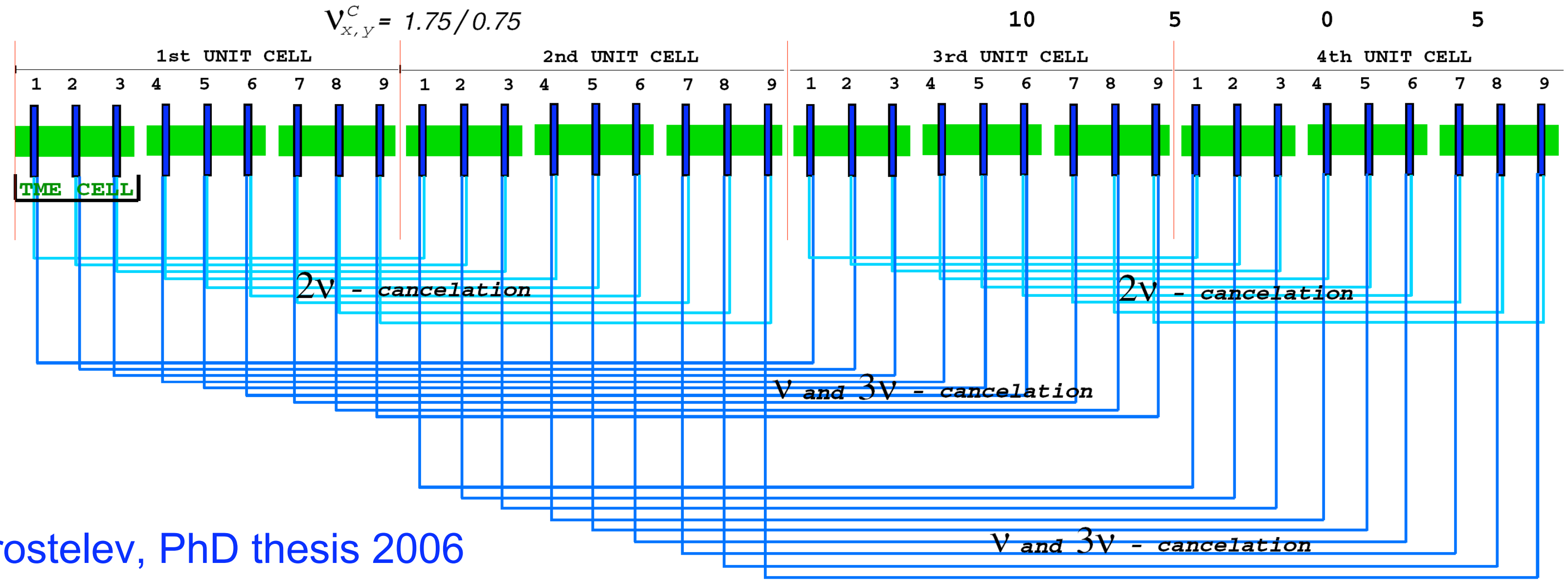

Korostelev, PhD thesis 2006

CLIC DR betatron tunes scan

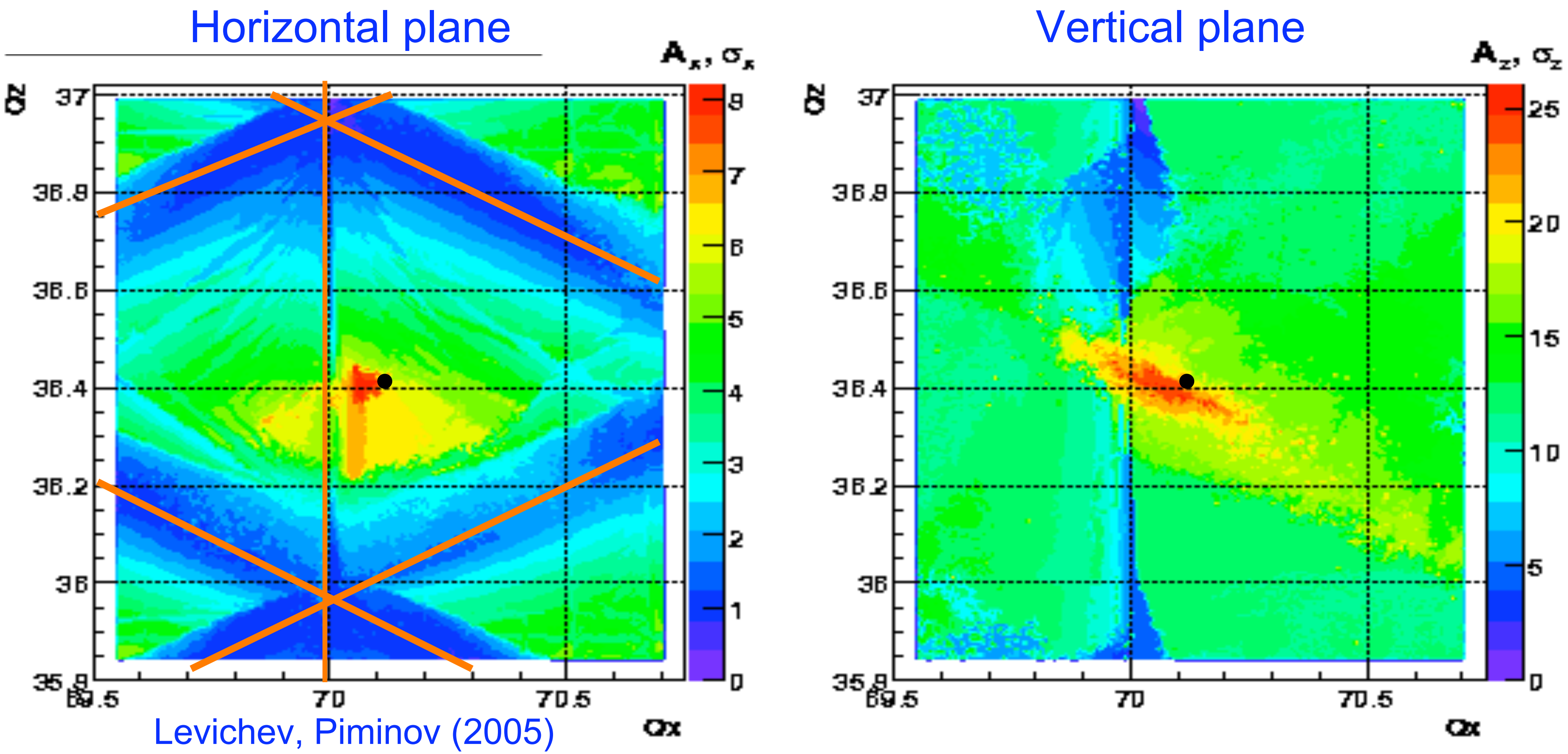

- Optimising the CLIC DR tune by scanning the tune space for maximum horizontal and vertical dynamic aperture
- DA limited by (1,±2) and integer resonance line

Effect of broken periodicity

Horizontal plane   Vertical plane   Levichev, Piminov (2005)

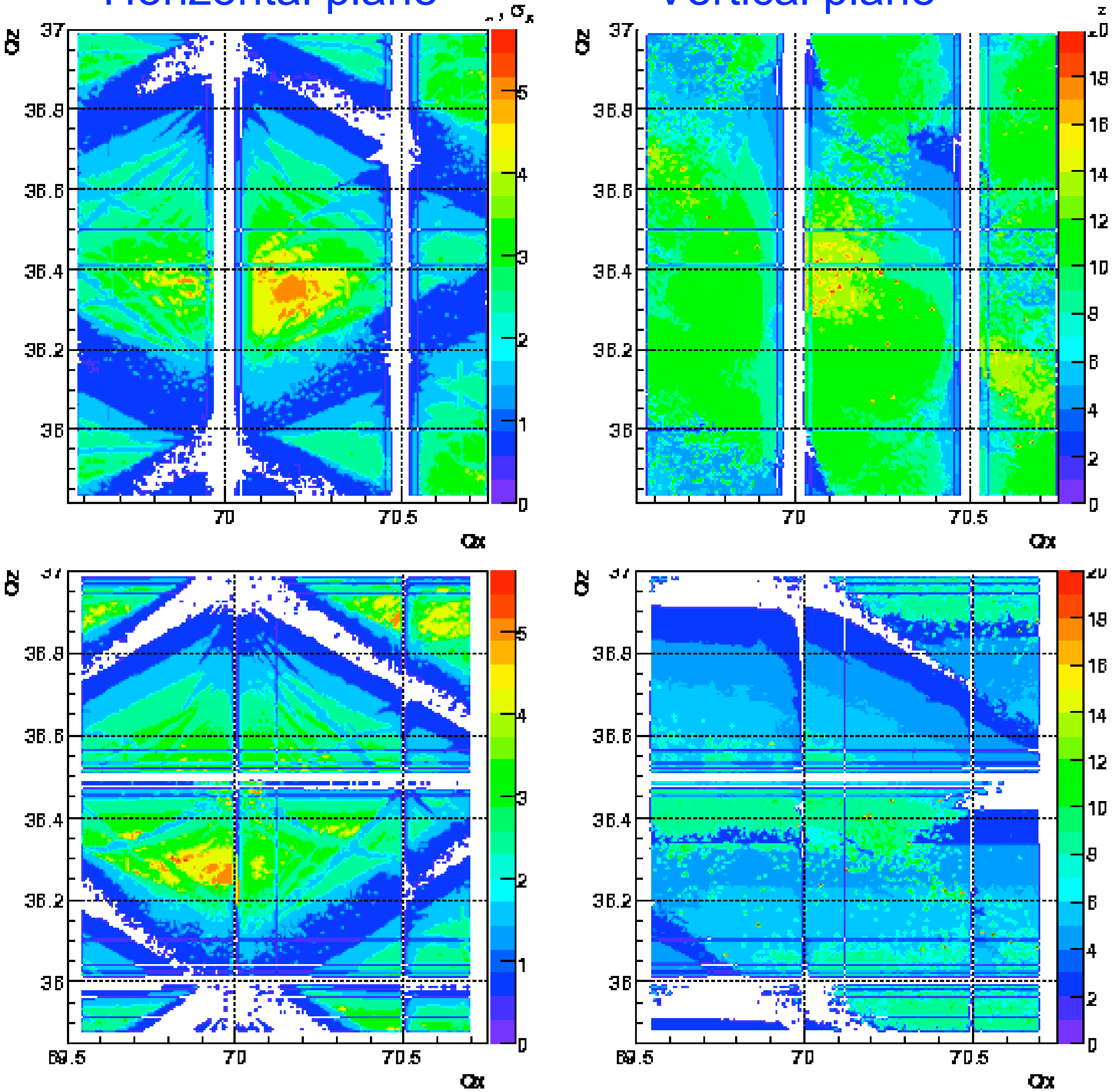

- With horizontal or vertical beta beating of 5%, appearance of large amount of non-systematic resonances, shrinking the DA and the optimal tune areas

DA for Damping wigglers

- Particles through 3D wiggler field tracked with symplectic integrator (Verlet scheme)
- Linear optics distortion corrected with quadrupole magnets in the dispersion suppressor

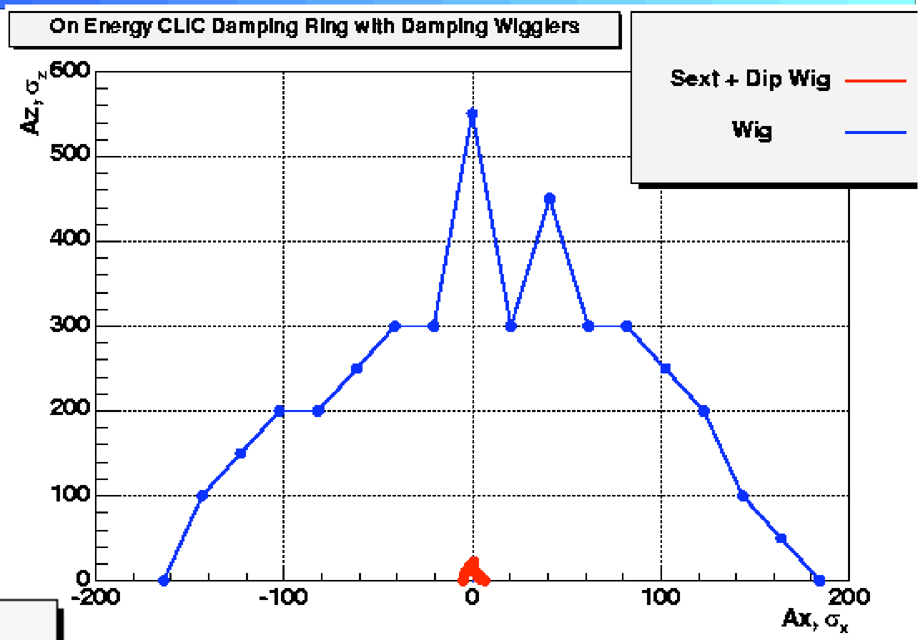

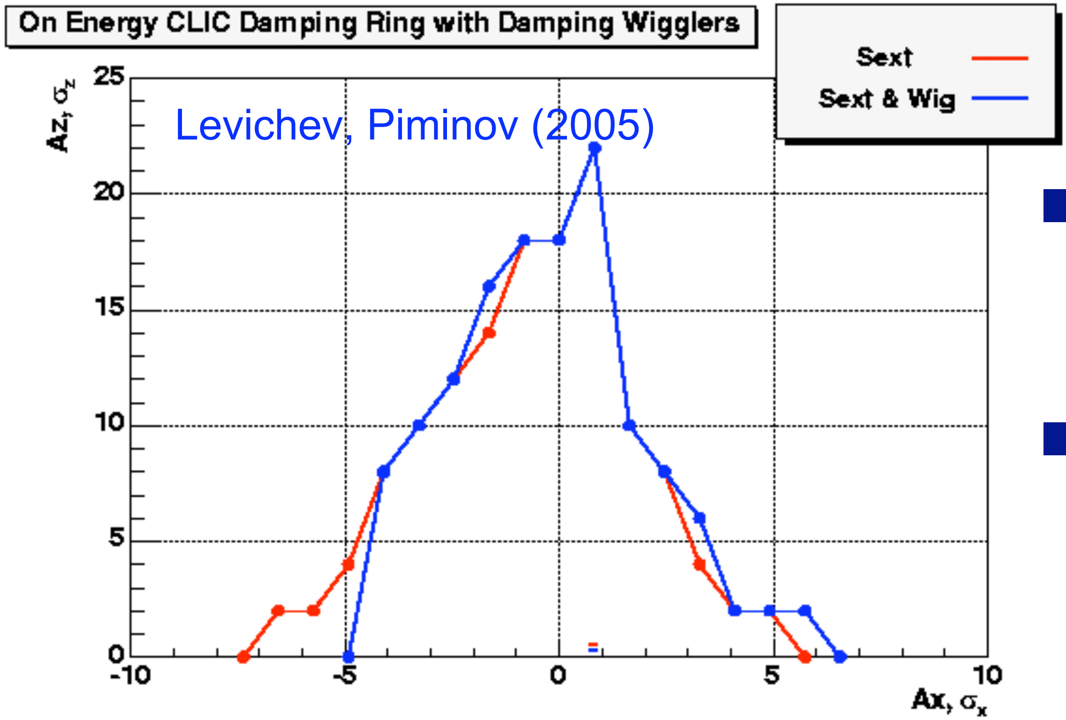

- Longitudinal field variation contributes to an octupole-like tune-spread
- Effect of wiggler in DA quite small

Effect of COD and coupling

- Several alignment errors considered introducing closed orbit distortion and dispersion variation
- Correction with dispersion free steering (orbit and dispersion correction)
- Skew quadrupole correctors for correcting dispersion in the arc and emittance minimisation
- Even after correction, reduction of the DA, especially in the vertical plane

Korostelev, Zimmermann (2006)

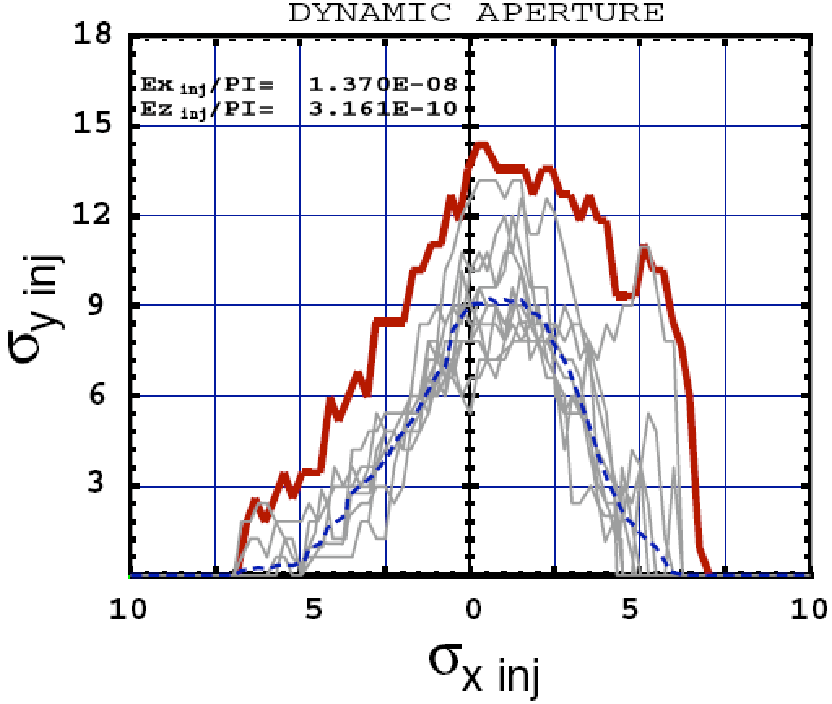

Imperfections	Simbol	1 r.m.s.
Quadrupole misalignment	$\langle \Delta Y_{\text{quad}} \rangle, \langle \Delta X_{\text{quad}} \rangle$	90 μm.
Sextupole misalignment	$\langle \Delta Y_{\text{sext}} \rangle, \langle \Delta X_{\text{sext}} \rangle$	40 μm
Quadrupole rotation	$\langle \Delta \Theta_{\text{quad}} \rangle$	100 μrad
Dipole rotation	$\langle \Delta \Theta_{\text{dipole arc}} \rangle$	100 μrad.
BPMs resolution	$\langle R_{\text{BPM}} \rangle$	2 μm.

Effect of radiation damping

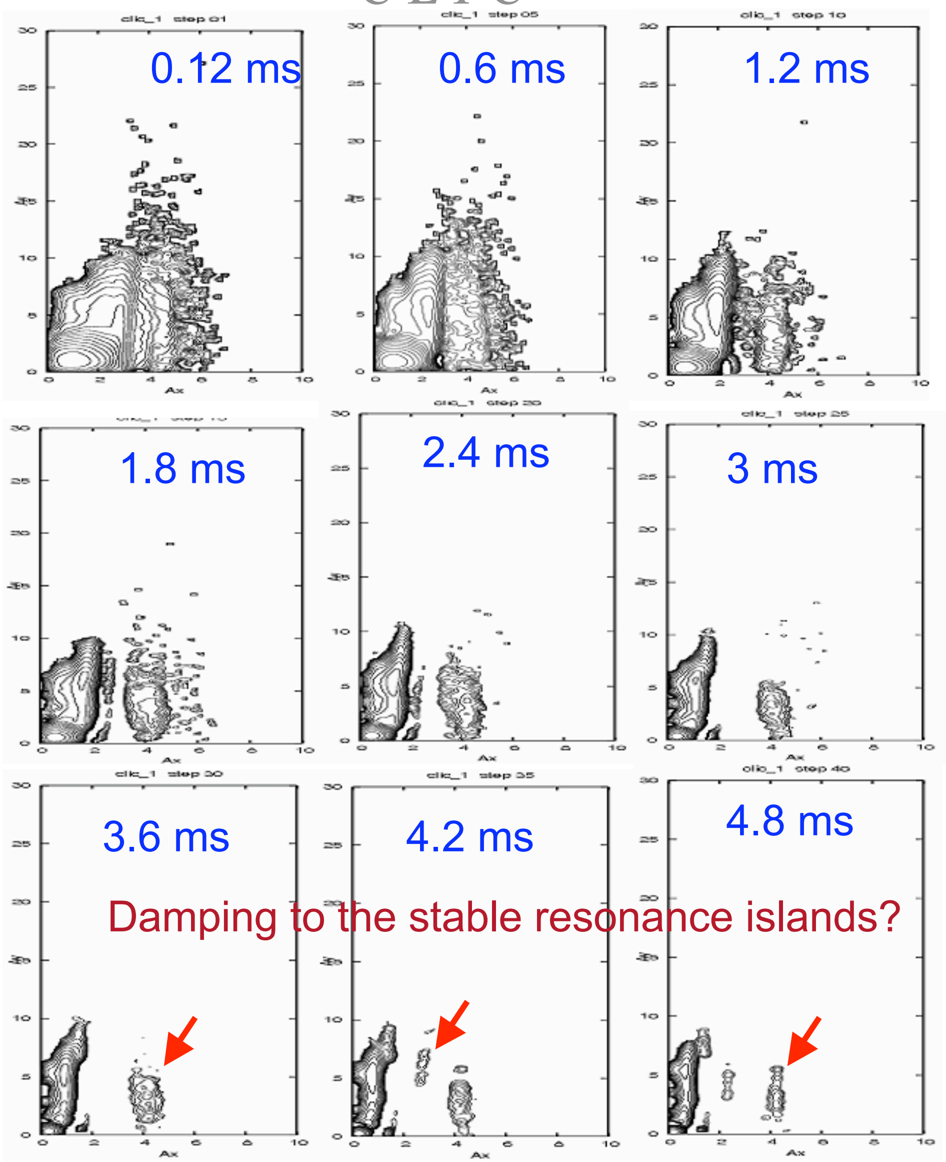

Levichev (2007)

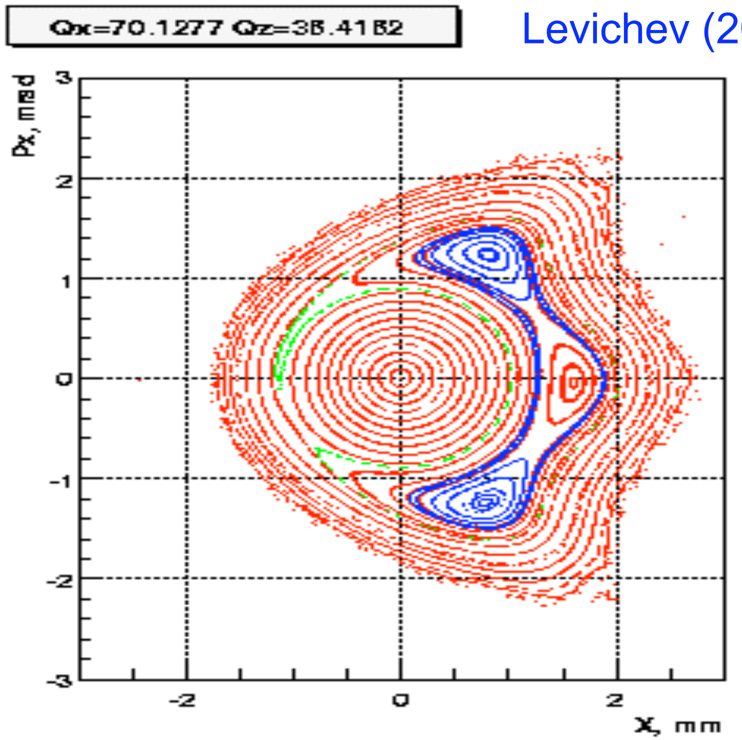

- Including radiation damping and excitation shows that 0.7% of the particles are lost during the damping
- Certain particles seem to damp away from the beam core, on resonance islands

Perspectives

- Optimise the TME cell for realistic magnet parameters
- Reiterate sextupole optimisation and non-linear dynamics including magnet and wiggler field errors
- Include space effect: in fact the space charge tune-shift at injection is negligible but when the beam shrinks it becomes quite large

$$\Delta\nu_y = \frac{N_{bp} r_0}{(2\pi)^{3/2}\gamma^3\sigma_s} \oint \frac{\beta_y}{\sigma_y(\sigma_x+\sigma_y)} ds \approx 0.15$$

  and should be taken into account at least in the tune optimisation
- Include effect of radiation damping, excitation and IBS in the non-linear optimisation process
- Use symplectic integrators + resonance analysis (frequency and diffusion maps)